Published in final edited form as:
Contrast Media Mol Imaging. 2014 July ; 9(4): 276–282. doi:10.1002/cmmi.1570.

Dynamic fluorescent imaging with indocyanine green for monitoring the therapeutic effects of photoimmunotherapy

Towhid Ali, **Takahito Nakajima**, **Kohei Sano**, **Kazuhide Sato**, **Peter L. Choyke**, and **Hisataka Kobayashi***
Molecular Imaging Program, Center for Cancer Research, National Cancer Institute, NIH, Bethesda, MD 20892-1088

Abstract

A new type of monoclonal antibody (mAb)-based, highly specific phototherapy (photoimmunotherapy; PIT) that uses a near infrared (NIR) phthalocyanine dye, IRDye700DX (IR700) conjugated with a mAb, has recently been described. NIR light exposure leads to immediate, target-selective necrotic cell death. However, tumor shrinkage takes several days to occur, making it difficult to detect earlier changes in the tumor. In this study, Panitumumab targeting the epidermal growth factor receptor (EGFR1) conjugated to IR700 was used to treat EGFR-expressing A431 tumor cells and in vivo xenografts. PIT was performed at varying doses of NIR light (10, 30, 50 and 100J/cm^2) in xenograft tumors in mice. Indocyanine green (ICG) dynamic imaging was evaluated for monitoring cytotoxic effects for the first hour after PIT. Our results demonstrated a statistical difference ($p<0.05$) in ICG intensity between control and PIT treated tumors in the higher light exposure groups (**50J/cm^2**: 2.94±0.35 vs. 5.22±0.92; p=0.02 and **100J/cm^2**: 3.56±0.96 vs. 5.71±1.43; p=0.008) as early as 20 minutes post ICG injection. However, no significant difference ($p>0.05$) in ICG intensity between control and PIT treated tumors was evident in the lower light exposure group at any time points up to 60mins **(10J/cm^2**: 1.92±0.49 vs. 1.71±0.3; p=0.44 and **30J/cm^2**: 1.57±0.35 vs. 2.75±0.59; p=0.07). Similarly, the retention index (background to corrected uptake ratio of ICG) varied with light exposure. In conclusion, ICG may serve as a potential indicator of acute cytotoxic effects of mAb-IR700-induced PIT even before morphological changes can be seen in targeted tumors.

Keywords

photoimmunothearpy; cancer fluorescence imaging; indocyanine green; super-enhanced permeability and retention effect

1. INTRODUCTION

Photoimmunotherapy (PIT) is a recently reported, highly selective cancer therapy (1). It utilizes a monoclonal antibody (mAb)-conjugated with a photosensitizing phthalocyanine dye, IRDye 700DX (700DX) to target and kill cancer cells after exposure to near infrared (NIR) light exposure. The mAb-700DX conjugate is only active as a therapeutic agent, when it is bound to the target cell membrane; otherwise it has no discernable effects on adjacent non-target-expressing cells. Following NIR light exposure, nearly immediate, target-

*Corresponding author: Hisataka Kobayashi, MD, PhD, Molecular Imaging Program, NCI/NIH, Bldg. 10, Room B3B69, MSC 1088, Bethesda, Maryland 20892-1088, USA, Kobayash@mail.nih.gov.

6. CONFLICT OF INTEREST

The authors declare that they have no conflict of interest.

selective necrotic cell death was observed *in vitro*. However, the *in vivo* assessment of rapid cell death is more challenging because morphological changes are slow to develop, requiring several days to become apparent. Progressive tumor shrinkage *in vivo* was observed 3–4 days after PIT, even after only a single administration of mAb-IR700 and a single exposure of NIR light, nonetheless there is uncertainty over how quickly cell death occurs in vivo (2). Real-time monitoring of PIT effects could be important for ascertaining whether a PIT session has been effective and whether additional cycles of therapy are needed (1). This might include additional doses of light, higher intensity light or additional doses of the mAb-IR700 conjugate or all of these. Immediate feedback is especially important during surgical or interventional procedures under endoscopy. However, no clinically applicable imaging technology exists for assessing real-time effects of PIT on site (3,4).

Indocyanine green (ICG) is an FDA approved NIR fluorescent dye that is known to reversibly bind serum proteins (ex: albumin). Therefore, ICG shows relatively high retention in the vascular pool after intravenous administration (5). PIT has been shown to induce cytotoxic effects in perivascular cancer cells leading to sudden necrosis and loss of vessel integrity resulting in a dramatic increase in vascular permeability, especially for macromolecules (6). This effect has been termed SUPR (super-enhanced permeability and retention), since a striking increase in permeability and retention of nanoparticles, is observed in newly treated tumors (7,8). ICG leakage into tumor was evaluated as an imaging biomarker for the evaluation of the acute therapeutic effects of PIT. We evaluate this method in the setting of monitoring of therapeutic effects *in vivo* immediately after PIT.

2. EXPERIMENTAL

2.1. Cell Lines and Culture

The EGFR positive cell line, A431 was used for EGFR targeting studies with panitumumab conjugates. The cell line was grown in RPMI 1640 (Life Technologies) containing 10% fetal bovine serum (Life Technologies), 0.03% L-glutamine, 100 units/mL penicillin, and 100 mg/mL streptomycin in 5% CO2 at 37C.

2.2. Reagents

Panitumumab, a fully humanized IgG2 mAb directed against the human epidermal growth factor receptor (EGFR), or HER1, was purchased from AMGEN Inc. A water soluble, silica-phthalocyanine derivative, IRDye 700DX NHS ester (IR700; C74H96N12Na4O27S6Si3, molecular weight of 1954.22) was purchased from LI-COR Bioscience. All other chemicals used were of reagent grade.

2.3. Synthesis of IR700-conjugated panitumumab

Panitumumab (1 mg, 6.8 nmol) was incubated with IR700 (66.8 mg, 34.2 nmol, 5 mmol/L in DMSO) in 0.1 mol/L Na2 HPO4 (pH 8.6) at room temperature for 1 hour. Then the mixture was purified with a Sephadex G50 column (PD-10; GE Healthcare). The protein concentrations were determined with Coomassie Plus Protein Assay Kit (Pierce Bio-technology) by measuring light absorption at 595 nm (8453 Value System; Agilent Technologies). The concentration of IR700 was measured by absorption with spectroscopy to confirm the average number of fluorophore molecules conjugated to each panitumumab molecule. The number of IR700 per antibody was approximately 4 for the 1: 5 reaction conditions. The addition of 0.4% SDS to the sample dissociated the fluorophores from each other, effectively causing dequenching. Quenching efficiency for a particular conjugation is defined as the fluorescence intensity with SDS divided by fluorescence intensity without SDS. Panitumumab-IR700 conjugate (Pan-IR700) showed a quenching efficiency of about 4.0 at pH 7.2. Pan-IR700 was kept at 4C in the refrigerator as a stock solution.

2.4. Mouse model and PIT for in vivo models

All in vivo procedures were conducted in compliance with the Guide for the Care and Use of Laboratory Animal Resources (1996), U.S. National Research Council, and approved by the National Cancer Institute/NIH Animal Care and Use Committee. Six-week-old to 8-week-old female homozygote athymic nude mice were purchased from Charles River (National Cancer Institute, Frederick). During treatment, mice were anesthetized with isoflurane. Two million A431 cells were injected subcutaneously in the right and left flanks of each mouse. Five days after cell injection, 100 μg of Pan-IR700 was administered intravenously, and 1 day later, one side was irradiated with NIR light from a red-light-emitting diode at wavelengths of 670–710 nm and a power density of 10, 30, 50 and100 J/cm^2, as measured with an optical power meter (PM 100, Thorlabs). The other side was shielded from light using aluminum foil. Immediately after finish exposing NIR light for PIT, 100 μL of ICG (0.1mM) was injected intravenously into all mice, and in vivo dynamic imaging studies were carried out for a duration of 60 min.

2.5. Dynamic In vivo ICG imaging studies after PIT

Immediately after PIT treatment, NIR ICG dynamic images were obtained consecutively for 60mins. In vivo fluorescence images of both IR700 and ICG were obtained with a Pearl Imager (LI-COR Biosciences) using the 700nm and 800nm fluorescence channels. Briefly, immediately after finished exposing to light with LED for PIT, all anesthetized mice were moved to an imaging bed with a nose corn, which was equipped with the Pearl Imager, for inhaling isoflurane and placed at a fixed position. After intravenous injection of ICG on the imaging bed, serial NIR fluorescence images were taken every one minute up to 60 min after ICG injection. Mean intensities of ICG of each ROI were calculated for tumors on both sides of the dorsum as well as the background.

2.6. Histologic analysis

To evaluate serial histologic changes correlating with dynamic ICG fluorescence imaging after PIT with various NIR light doses, microscopic study was conducted (BX61, Olympus America). A431 tumors treated with PIT by exposing 0, 10, 30, 50 and 100 J/cm^2 of NIR light were harvested in 10% formalin immediately after finishing dynamic fluorescence imaging study. Serial three 10-mm slice sections were fixed on a glass slide with H&E staining.

2.7. Statistical analysis

Statistical analyses were carried out using a statistics program (GraphPad Prism, GraphPad Software. Student *t*-test (unpaired) was used to compare the average values of each treatment groups between those of PIT-treated tumors and untreated tumors at each 10 min interval until 60mins. Student *t*-test (paired) was also used to compare the PIT TBR of ICG between 1min to 60min p.i in each light exposure group. Mann-Whitney's *U* test was used to compare the retention index value between the different light exposure groups at 20min intervals. $p<0.05$ was considered to indicate a statistically significant difference.

3. RESULTS

3.1 *In vivo* Dynamic Imaging of ICG after Pan-IR700 mediated PIT

A rapid accumulation of ICG was observed in the higher light dose PIT-treated tumors (50 and 100J/cm^2) immediately after injection vs. the lower light dose PIT-treated tumors (10 and 30J/cm^2). In addition, all groups demonstrated no or minimal uptake of ICG in the control tumors (Figure 1). In the lower light exposure groups (10 and 30J/cm^2, Figure 2B), ICG light signal intensity (SI) gradually decreased post-injection (p.i) while at the higher

light exposures (50 and 100J/cm^2), ICG SI rapidly increased immediately p.i, peaking at ~30 min before plateauing (Figure 2A).

3.2. Greater exposure of NIR light led to a difference in ICG Signal Intensity

The higher light exposure group demonstrated a significant difference ($p<0.05$) in ICG SI between PIT-treated tumors and control tumors reflected by a 2.1-fold and 2.3-fold higher ICG SI in 100J/cm^2 (5.30±1.39 vs. 2.50±0.62; p=0.012) and 50J/cm^2 (4.74±0.91 vs. 2.05±0.25; p=0.017) groups respectively at 60mins (Figure 2A). This effect is seen as early as 20mins p.i at 50J/cm^2 (5.22±0.92 vs. 2.94±0.35; p=0.02) and even earlier at 10 min p.i. for 100J/cm^2 (5.37±1.17 vs. 4.22±1.12; p=0.02). In both groups, the difference between the PIT-treated tumors and control tumors was maintained up for 60mins ($p<0.05$). In addition, it was observed that there was no significant difference ($p>0.05$) in ICG SI in the lower exposure group between PIT-treated tumors and controls at any time-point during the 60 min interval as there was less than a 2-fold difference in both treatment groups (Figure 2B). Comparing only the ICG SIs of PIT-treated tumors to each other, both of the higher light exposure groups were significantly different ($p<0.05$) from the lowest light exposure group of 10J/cm^2 starting at 20 min and continuing to 60mins (Figure 3). When comparing the higher light doses directly to the lower light doses, starting at 10mins p.i, 100J/cm^2 (5.37±1.17) was at least more than 1.5-fold higher than both 30J/cm^2 (3.53±0.70) and 10J/cm^2 (2.68±0.34) and subsequently increased by the end of 60mins to more than 1.9-fold (30J/cm^2) and 3-fold higher (10J/cm^2), respectively. Similarly, 50J/cm^2 (4.94±0.9) was at least 1.4-fold higher than both 30J/cm^2 (3.53±0.7) and 10J/cm^2 (2.68±0.34) starting at 10mins and by the end of 60mins was more than 1.7-fold (30J/cm^2) and 2.8-fold higher (10J/cm^2), respectively.

In addition, when comparing 1 to 60 min p.i of ICG, the average PIT tumor-to-background ratio (TBR) was significantly increased in the higher light exposure group (100 and 50J/cm^2; p=0.00007 and p=0.007, respectively) and ICG accumulation can be clearly seen in the PIT-treated tumors reflecting the very high TBR (TBR_{60min} =3.42 ±0.28 and TBR_{60min} =3.24±0.55, respectively). In the lower light exposure groups there was no significant difference observed when comparing 1 to 60 min p.i of ICG (**10J/cm^2**: TBR_{1min}=1.48±0.22 vs. TBR_{60min}=1.74±0.47; p=0.35 & **30J/cm^2**: TBR_{1min}=1.53±0.12 vs. TBR_{60min}=2.35±0.47; p=0.07).

3.3. Retention index of ICG

To further quantitate our observation, we investigated the background-corrected uptake ratio of ICG (or retention index) at 60 min using the following equation: [(SIPIT at 60 min - SIBackground at 60 min) - (SIPIT at 1 min - SIBackground at 1 min)]/[(SIControl at 60 min - SIBackground at 60 min) - (SIControl at 1 min - SIBackground at 1 min)]. This was also done at 20 and 40 min. No significant difference ($p>0.05$)was seen at 20, 40 or 60 min in the retention of ICG when comparing the two higher light exposure groups (100J and 50J/cm^2) to each other (11.02±5.6, 18.32±15.2, 11.21±8.1 vs. 25.24±12.1, 13.46±5.0, 16.92±7.1 respectively). Additionally, the higher light exposure group was significantly different ($p<0.05$) to the lower light exposure groups and this is best seen at 40 min [18.32 ±15.2 (100J/cm^2), 13.46 ±5.0 (50J/cm^2), 0.83 ±0.45 (30J/cm^2), 0.42±0.23 (10J/cm^2)] (Figure 4).

3.4. Histologic analysis

Microscopic evaluation of PIT treated tumors revealed diffuse necrosis and micro-hemorrhage with scattered clusters of damaged tumor cells after PIT with 50–100J/cm^2. Necrotic damage was more intense and fewer tumor cells remained, when higher energy (100J/cm^2) NIR light was administered (Figure 5). In histological findings, cancer cell

damages are well correlated with increased enhancement of tumor tissue with ICG shown in dynamic fluorescence imaging.

4. DISCUSSION

Near-infrared (NIR) fluorescent imaging has emerged as a potential tool for *in vivo* tumor imaging. It is non-invasive, does not involve ionizing radiation and is relatively portable and inexpensive (5). ICG, a NIR fluorescent dye, is one of two fluorescent contrast agents approved by the FDA for clinical applications and has a long history of use in humans with an excellent safety profile. It has been used clinically in hepatic clearance studies, cardiovascular function testing and retinal angiography (9,10). Recently, ICG has been increasingly used in the operating room for various image-guided oncologic surgical procedures. For example, ICG has been utilized for sentinel lymph node mapping in multiple cancers showing excellent results in breast and skin cancer (11–21). Because it is exclusively excreted into the bile, it has been used for the real time visualization of the biliary tree during cholecystectomy and other hepatobiliary surgery (22–25). Furthermore, pathology that disrupts biliary excretion and the hypervascularity of certain tumors has allowed imaging of hepatobiliary cancer including colorectal metastasis, hepatocellular carcinoma and cholangiocarcinoma (26–30). Other studies have also shown that it was possible using ICG to identify extrahepatic metastasis of hepatocellular carcinoma (31), hepatic micrometastases of pancreatic cancer (32), haemangioblastomas (33), head and neck cancer (34) as well as for colonic tattooing of colorectal cancer (35–37) and the assessment of anastomotic perfusion during colorectal surgery (38,39). In addition, ICG has been used in angiography for reconstructive surgery after oncologic surgery (40–43). It is known that ICG molecules bind reversibly to serum proteins in the blood such as albumin which reduces aggregation, while increasing brightness by over 3-fold and the effective hydrodynamic diameter to approximately 7nm. The latter has important implications for the biodistribution and pharmacokinetics of ICG in vivo (5,44,45).

Permeability and retention of ICG in PIT-treated tumors and control tumors were compared. After PIT, a super enhanced permeability and retention is observed in the treated area, a phenomenon termed SUPR. In A431 (EGFR positive)-bearing mice treated with Pan-IR700 PIT, accumulation of Pan-IR700 was detected in the perivascular tumor, and a gradient of IR700 fluorescence signals was observed depending on the distance from blood vessels. Having previously established that light exposure of 50J/cm^2 is sufficient to induce cell death in xenografts, four groups (≥ 5mice in each group) exposed to varying NIR light intensities (10, 30, 50 and 100J/cm^2) and were subsequently imaged with ICG. Ten mice were initially prepared for each light exposure group, however, mice were subsequently removed from data analysis for any of the following reasons: tumors were asymmetrical or the mice moved or died during dynamic imaging due to anesthesia effects. In each mouse with bilateral tumors, only unilateral light exposure was performed, while the contralateral tumor was shielded from light. All the treated tumors had a volume ranging from 125 to 250 mm^3, with less than 25% volume difference between control and treated tumors. Our prior experiments with Pan-IR800 suggested that the optimal time to achieve maximal concentration of nanomaterials within the tumor is 1h after PIT (6). Hence ICG was administered intravenously and in vivo dynamic imaging studies were subsequently carried out for 1h.

Treatment with 50 and 100J/cm^2 of light led to the permeability and retention of ICG in the treated cancer. PIT with lower doses of NIR light (10 and 30J/cm^2) did not show significant ($p>0.05$) accumulation of ICG compared to control tumors in vivo. Hence the accumulation of ICG was dependent on the dose of NIR light exposure. This suggests that there is a threshold of light intensity that results in perivascular cell death leading to the SUPR effect,

which is reflected in increased enhancement on ICG studies. The retention index data also suggests that light exposure at 50J/cm^2 is optimal for inducing permeability and retention. This data also support previous work that demonstrates that 50J/cm^2 is a therapeutic dose and sufficient for inducing the SUPR effect consistent with prior work (2,6) while avoiding higher light doses that can induce unwanted side effects related to thermal effects.

Permeability and retention of ICG was observed within minutes after a single effective dose of NIR light, which indicated a biologic effect several days prior to the appearance of changes in tumor size. Lesion size is often a delayed indicator of tumor response, even though it is still used clinically. Uptake and retention of ICG is especially important in the setting of PIT, where light can be reapplied if necessary. Hence a more immediate readout of cell death will be clinically desired especially for surgical or endoscopic procedures where it is preferable to complete treatments during one procedure. ICG, which provides an immediate readout of the tumor's condition, can assess the therapeutic effects of PIT immediately after treatment and aids in deciding whether additional doses of NIR light exposure are necessary. Furthermore, our data illustrates the feasibility of using ICG clinically, given that it is FDA approved and widely available.

5. CONCLUSIONS

Intravenous ICG is a potential method of assessing the acute cytotoxic effects or vascular permeability effects of PIT using a mAb-IR700 conjugate, during surgical or endoscopic procedures. Successful PIT treatment induces the super-enhanced permeability and retention (SUPR effect) causing ICG bound to albumin to extravasate rapidly into the treated tumor bed. ICG accumulation and retention is optimal after 30–40 min post-injection and hence may be feasible for the real-time monitoring of PIT effects. Such monitoring could be important to assess whether a PIT session has been effective and whether additional cycles of therapy are needed. Moreover, it may indicate that adjuvant chemotherapies may be advantageous as doses can be reduced after PIT due to preferential leakage within the tumor bed. Thus, ICG imaging allows the assessment of the effect of PIT before morphological changes become evident in targeted tumors.

Acknowledgments

This research was supported by the Intramural Research Program of the National Institutes of Health, National Cancer Institute, Center for Cancer Research. This research was made possible through the National Institutes of Health (NIH) Medical Research Scholars Program, a public-private partnership supported jointly by the NIH and generous contributions to the Foundation for the NIH from Pfizer Inc, The Leona M. and Harry B. Helmsley Charitable Trust, and the Howard Hughes Medical Institute, as well as other private donors. For a complete list, please visit the Foundation website at http://www.fnih.org/work/programs-development/medical-research-scholars-program.

REFERNCES

1. Mitsunaga M, Ogawa M, Kosaka N, Rosenblum LT, Choyke PL, Kobayashi H. Cancer cell-selective in vivo near infrared photoimmunotherapy targeting specific membrane molecules. Nat Med. 2011; 17(12):1685–91. [PubMed: 22057348]
2. Mitsunaga M, Nakajima T, Sano K, Choyke PL, Kobayashi H. Near-infrared theranostic photoimmunotherapy (PIT): repeated exposure of light enhances the effect of immunoconjugate. Bioconj Chem. 2012; 23(3):604–9.
3. Young MR, Ileva LV, Bernardo M, Riffle LA, Jones YL, Kim YS, Colburn NH, Choyke PL. Monitoring of tumor promotion and progression in a mouse model of inflammation-induced colon cancer with magnetic resonance colonography. Neoplasia. 2009; 11(3):237–46. [PubMed: 19242605]

4. Kosaka N, Ogawa M, Choyke PL, Kobayashi H. Clinical implications of near-infrared fluorescence imaging in cancer. Future Oncol. 2009; 5(9):1501–11. [PubMed: 19903075]
5. Schaafsma BE, Mieog JSD, Hutteman M, Van der Vorst JR, Kuppen PJK, Löwik CWGM, Frangioni JV, Van de Velde CJH, Vahrmeijer AL. The clinical use of indocyanine green as a near-infrared fluorescent contrast agent for image-guided oncologic surgery. J Surg Oncol. 2011; 104(3): 323–32. [PubMed: 21495033]
6. Sano K, Nakajima T, Choyke PL, Kobayashi H. Markedly enhanced permeability and retention effects induced by photo-immunotherapy of tumors. ACS Nano. 2013; 7(1):717–24. [PubMed: 23214407]
7. Hagen A, Grosenick D, Macdonald R, Rinneberg H, Burock S, Warnick P, Poellinger A, Schlag PM. Late-fluorescence mammography assesses tumor capillary permeability and differentiates malignant from benign lesions. Opt Express. 2009; 17(19):17016–33. [PubMed: 19770920]
8. Mitsuhashi N, Kimura F, Shimizu H, et al. Usefulness of intraoperative fluorescence imaging to evaluate local anatomy in hepatobiliary surgery. J Hepatobiliary Pancreat Surg. 2008; 15(5):508–14. [PubMed: 18836805]
9. Sakka SG. Assessing liver function. Curr Opin Crit Care. 2007; 13(2):207–14. [PubMed: 17327744]
10. Dzurinko VL, Gurwood AS, Price JR. Intravenous and indocyanine green angiography. Optometry. 2004; 75(12):743–55. [PubMed: 15624671]
11. Troyan SL, Kianzad V, Gibbs-Strauss SL, Gioux S, Matsui A, Oketokoun R, Ngo L, Khamene A, Azar F, Frangioni JV. The FLARE intraoperative near-infrared fluorescence imaging system: a first-in-human clinical trial in breast cancer sentinel lymph node mapping. Ann Surg Oncol. 2009; 16(10):2943–52. [PubMed: 19582506]
12. Yamashita S, Tokuishi K, Anami K, et al. Video-assisted thoracoscopic indocyanine green fluorescence imaging system shows sentinel lymph nodes in non-small-cell lung cancer. J Thorac Cardiovasc Surg. 2011; 141(1):141–4. [PubMed: 20392454]
13. Murawa D, Hirche C, Dresel S, Hünerbein M. Sentinel lymph node biopsy in breast cancer guided by indocyanine green fluorescence. Br J Surg. 2009; 96(11):1289–94. [PubMed: 19847873]
14. Tagaya N, Aoyagi H, Nakagawa A, Abe A, Iwasaki Y, Tachibana M, Kubota K. A novel approach for sentinel lymph node identification using fluorescence imaging and image overlay navigation surgery in patients with breast cancer. World J Surg. 2011; 35(1):154–8. [PubMed: 20931198]
15. Fujiwara M, Mizukami T, Suzuki A, Fukamizu H. Sentinel lymph node detection in skin cancer patients using real-time fluorescence navigation with indocyanine green: preliminary experience. J Plast Reconstr Aesthet Surg. 2009; 62(10):e373–8. [PubMed: 18556255]
16. Tanaka R, Nakashima K, Fujimoto W. Sentinel lymph node detection in skin cancer using fluorescence navigation with indocyanine green. J Dermatol. 2009; 36(8):468–70. [PubMed: 19691754]
17. Tsujino Y, Mizumoto K, Matsuzaka Y, Niihara H, Morita E. Fluorescence navigation with indocyanine green for detecting sentinel nodes in extramammary Paget's disease and squamous cell carcinoma. J Dermatol. 2009; 36(2):90–4. [PubMed: 19284452]
18. Tajima Y, Murakami M, Yamazaki K, Masuda Y, Kato M, Sato A, Goto S, Otsuka K, Kato T, Kusano M. Sentinel node mapping guided by indocyanine green fluorescence imaging during laparoscopic surgery in gastric cancer. Ann Surg Oncol. 2010; 17(7):1787–93. [PubMed: 20162462]
19. Kusano M, Tajima Y, Yamazaki K, Kato M, Watanabe M, Miwa M. Sentinel node mapping guided by indocyanine green fluorescence imaging: a new method for sentinel node navigation surgery in gastrointestinal cancer. Dig Surg. 2008; 25(2):103–8. [PubMed: 18379188]
20. Sugie T, Sawada T, Tagaya N, Kinoshita T, Yamagami K, Suwa H, Ikeda T, Yoshimura K, Niimi M, Shimizu A, Toi M. Comparison of the Indocyanine Green Fluorescence and Blue Dye Methods in Detection of Sentinel Lymph Nodes in Early-stage. Breast Cancer Ann Surg Oncol. 2013; 20(7):2213–8.
21. Takeuchi M, Sugie T, Abdelazeem K, Kato H, Shinkura N, Takada M, Yamashiro H, Ueno T, Toi M. Lymphatic mapping with fluorescence navigation using indocyanine green and axillary surgery in patients with primary breast cancer. Breast J. 2012; 18(6):535–41. [PubMed: 23009222]

22. Ishizawa T, Tamura S, Masuda K, Aoki T, Hasegawa K, Imamura H, Beck Y, Kokudo N. Intraoperative fluorescent cholangiography using indocyanine green: a biliary road map for safe surgery. J Am Coll Surg. 2009; 208(1):e1–4. [PubMed: 19228492]
23. Ishizawa T, Bandai Y, Ijichi M, Kaneko J, Hasegawa K, Kokudo N. Fluorescent cholangiography illuminating the biliary tree during laparoscopic cholecystectomy. Br J Surg. 2010; 97(9):1369–77. [PubMed: 20623766]
24. Verbeek FPR, Van der Vorst JR, Schaafsma BE, Hutteman M, Bonsing BA, Van Leeuwen FWB, Frangioni JV, Van de Velde CJH, Swijnenburg R-J, Vahrmeijer AL. Image-guided hepatopancreatobiliary surgery using near-infrared fluorescent light. J Hepatobiliary Pancreat Sci. 2012; 19(6):626–37. [PubMed: 22790312]
25. Aoki T, Murakami M, Yasuda D, et al. Intraoperative fluorescent imaging using indocyanine green for liver mapping and cholangiography. J Hepatobiliary Pancreat Sci. 2010; 17(5):590–4. [PubMed: 19844652]
26. Ishizawa T, Fukushima N, Shibahara J, Masuda K, Tamura S, Aoki T, Hasegawa K, Beck Y, Fukayama M, Kokudo N. Real-time identification of liver cancers by using indocyanine green fluorescent imaging. Cancer. 2009; 115(11):2491–504. [PubMed: 19326450]
27. Ishizawa T, Bandai Y, Harada N, Muraoka A, Ijichi M, Kusaka K, Shibasaki M, Kokudo N. Indocyanine green-fluorescent imaging of hepatocellular carcinoma during laparoscopic hepatectomy: An initial experience. Asian J Endosc Surg. 2010; 3(1):42–45.
28. Uchiyama K, Ueno M, Ozawa S, Kiriyama S, Shigekawa Y, Yamaue H. Combined use of contrast-enhanced intraoperative ultrasonography and a fluorescence navigation system for identifying hepatic metastases. W J Surg. 2010; 34(12):2953–9.
29. Harada N, Ishizawa T, Muraoka A, Ijichi M, Kusaka K, Shibasaki M, Yamamoto K, Hasegawa K, Bandai Y, Kokudo N. Fluorescence navigation hepatectomy by visualization of localized cholestasis from bile duct tumor infiltration. J Am Coll Surg. 2010; 210(6):e2–6. [PubMed: 20510795]
30. Gotoh K, Yamada T, Ishikawa O, Takahashi H, Eguchi H, Yano M, Ohigashi H, Tomita Y, Miyamoto Y, Imaoka S. A novel image-guided surgery of hepatocellular carcinoma by indocyanine green fluorescence imaging navigation. J Surg Oncol. 2009; 100(1):75–9. [PubMed: 19301311]
31. Satou S, Ishizawa T, Masuda K, Kaneko J, Aoki T, Sakamoto Y, Hasegawa K, Sugawara Y, Kokudo N. Indocyanine green fluorescent imaging for detecting extrahepatic metastasis of hepatocellular carcinoma. J Gastroenterol. 2012 in press. 10.1007/s00535-012-0709-6
32. Yokoyama N, Otani T, Hashidate H, Maeda C, Katada T, Sudo N, Manabe S, Ikeno Y, Toyoda A, Katayanagi N. Real-time detection of hepatic micrometastases from pancreatic cancer by intraoperative fluorescence imaging: preliminary results of a prospective study. Cancer. 2012; 118(11):2813–9. [PubMed: 21990070]
33. Benedetto N, Aquila F, Vannozzi R. Use of near-infrared indocyanine videoangiography and Flow 800 in the resectioning of a spinal cord haemangioblastoma. Br J Neurosurg. 2013 in press. 10.3109/02688697.2013.798863
34. Yokoyama J, Fujimaki M, Ohba S, Anzai T, Yoshii R, Ito S, Kojima M, Ikeda K. A feasibility study of NIR fluorescent image-guided surgery in head and neck cancer based on the assessment of optimum surgical time as revealed through dynamic imaging. Onco Targets Ther. 2013; 6:325–30. [PubMed: 23630424]
35. Hammond DC, Lane FR, Mackeigan JM, Passinault WJ. Endoscopic tattooing of the colon: clinical experience. Am Surg. 1993; 59(3):205–10. [PubMed: 8476162]
36. Miyoshi N, Ohue M, Noura S, et al. Surgical usefulness of indocyanine green as an alternative to India ink for endoscopic marking. Surg Endosc. 2009; 23(2):347–51. [PubMed: 18443867]
37. Watanabe M, Tsunoda A, Narita K, Kusano M, Miwa M. Colonic tattooing using fluorescence imaging with light-emitting diode-activated indocyanine green: a feasibility study. Surg Today. 2009; 39(3):214–8. [PubMed: 19280280]
38. Kudszus S, Roesel C, Schachtrupp A, Höer JJ. Intraoperative laser fluorescence angiography in colorectal surgery: a noninvasive analysis to reduce the rate of anastomotic leakage. Langenbecks Arch Surg. 2010; 395(8):1025–30. [PubMed: 20700603]

39. Sherwinter DA, Gallagher J, Donkar T. Intra-operative transanal near infrared imaging of colorectal anastomotic perfusion: a feasibility study. Colorectal Dis. 2013; 15(1):91–6. [PubMed: 22632448]
40. Lee BT, Matsui A, Hutteman M, Lin SJ, Winer JH, Laurence RG, Frangioni JV. Intraoperative near-infrared fluorescence imaging in perforator flap reconstruction: current research and early clinical experience. J Reconstr Microsurg. 2010; 26(1):59–65. [PubMed: 20027541]
41. Betz CS, Zhorzel S, Schachenmayr H, Stepp H, Havel M, Siedek V, Leunig A, Matthias C, Hopper C, Harreus U. Endoscopic measurements of free-flap perfusion in the head and neck region using red-excited Indocyanine Green: preliminary results. J Plastic Reconstr Aesthet Surg. 2009; 62(12): 1602–8.
42. Newman MI, Samson MC. The application of laser-assisted indocyanine green fluorescent dye angiography in microsurgical breast reconstruction. J Reconstr Microsurg. 2009; 25(1):21–6. [PubMed: 18925547]
43. Komorowska-Timek E, Gurtner GC. Intraoperative perfusion mapping with laser-assisted indocyanine green imaging can predict and prevent complications in immediate breast reconstruction. Plast Reconstr Surg. 2010; 125(4):1065–73. [PubMed: 20335859]
44. Landsman ML, Kwant G, Mook GA, Zijlstra WG. Light-absorbing properties, stability, and spectral stabilization of indocyanine green. J Appl Physiol. 1976; 40(4):575–83. [PubMed: 776922]
45. Yoneya S, Saito T, Komatsu Y, Koyama I, Takahashi K, Duvoll-Young J. Binding properties of indocyanine green in human blood. Invest Ophthalmol Vis Sci. 1998; 39(7):1286–90. [PubMed: 9620093]

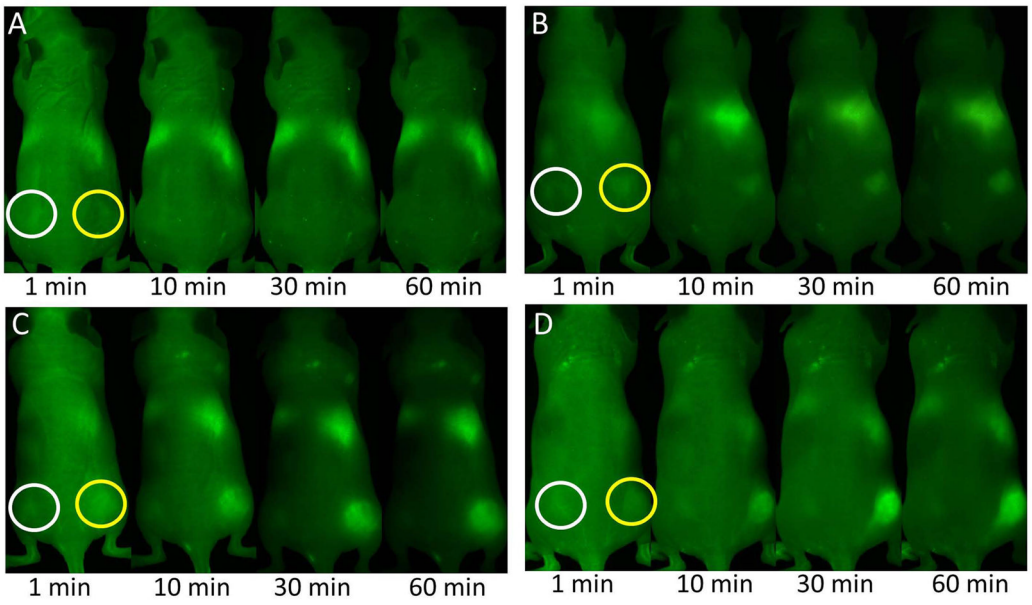

Figure 1.

Dynamic images obtained after ICG administration at 1 min, 10min, 30min and 60min post-injection. ICG: green. A) 10J/cm^2 light treatment group, B) 30J/cm^2 light treatment group C) 50J/cm^2 light treatment group D) 100J/cm^2 light treatment group. These images show the rapid accumulation of ICG in the PIT-treated tumors (yellow circles) while minimal or no accumulation in the control tumors (white circles). At 60mins the tumor-to-background (TRB) ratio is dramatically increased for the higher light exposure groups.

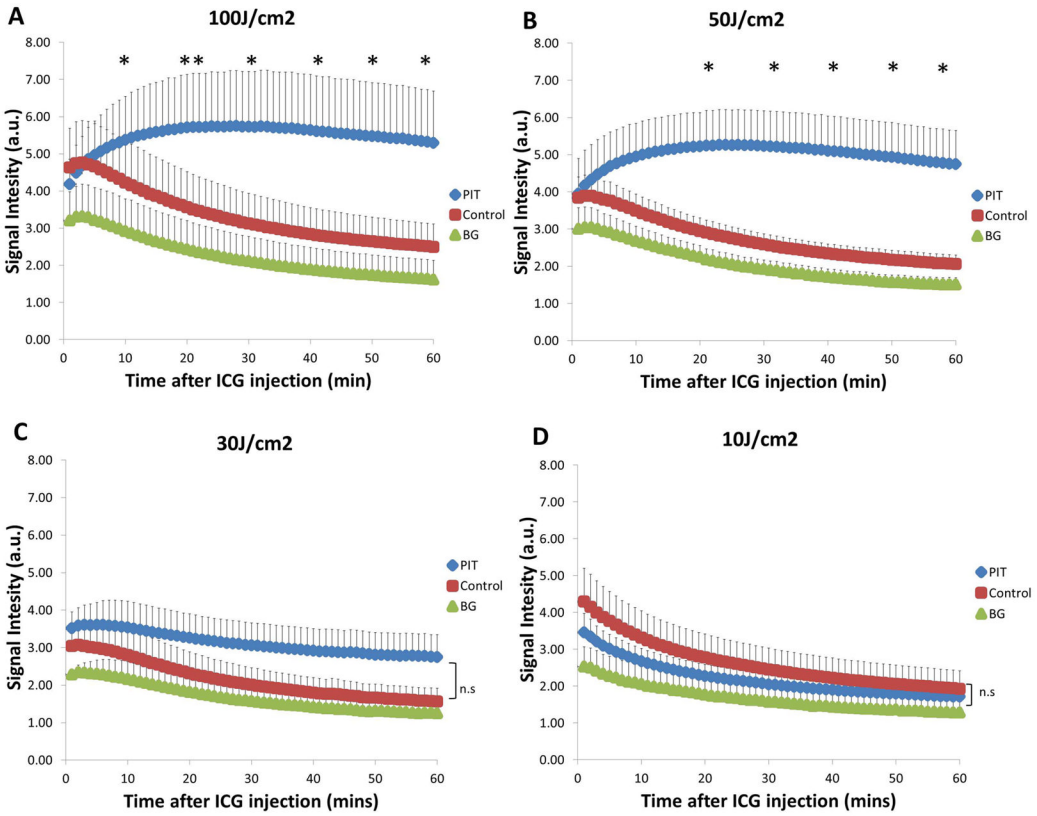

Figure 2.

ICG Signal Intensity (SI) of higher light exposure groups A) 100J/cm^2 and B) 50J/cm^2. Mean ICG SI was calculated using the values of all mice in each treatment group. ICG SI was then compared between PIT-treated tumor and control tumors. A significant difference of ICG SI can be seen between PIT-treated tumors and control tumors as soon as 20mins p.i and even earlier at 10mins p.i at the highest light exposure group. PIT-treated tumors were 2.1-fold and 2.3-fold higher than control tumors in 100J and 50J/cm^2 treatment group, respectively. Higher light exposure of at least 50J/cm^2 is sufficient to induce the SUPR effect resulting in the accumulation of ICG in PIT-treated tumors. This may indicate early changes after successful PIT treatment. ICG Signal Intensity (SI) of lower light exposure groups C) 30J/cm^2 and D) 10J/cm^2. No significant difference of ICG SI can be seen between PIT-treated tumors and control tumors at any timepoints. This suggests that at such a low light exposure dose, PIT is ineffective to induce the SUPR effect hence there is minimal difference in ICG SI between PIT-treated tumors and control tumors. Data are means ± SEM (n=6 for A and B, n=5 for C and D). (***** $p<0.05$, ****** $p<0.01$, ns= not significant)

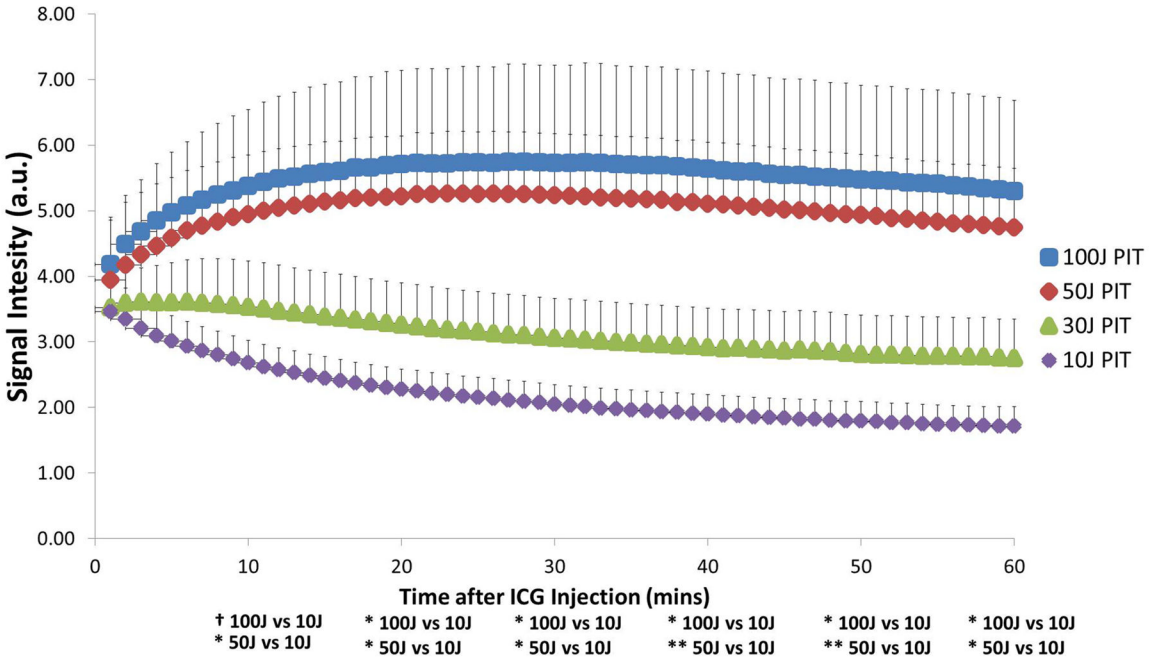

Figure 3.

ICG Signal Intensity (SI) of PIT-treated tumors for each treatment group. Significant difference of ICG SI was calculated between each group. When comparing the higher exposure groups to the lower exposure groups, it is noticed that starting at 10mins, ICG SI was at least 1.4-fold higher and by the end of imaging (60mins) had increased to at least 2.8-fold higher. Data are means ± SEM (n≥5) Key: ***** $p<0.05$, ****** $p<0.01$, **†** - marginally significant

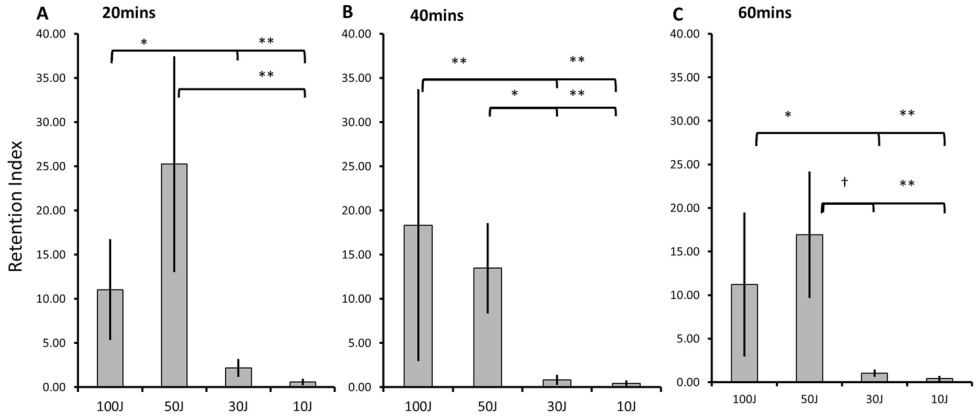

Figure 4.

Retention index of ICG at 20-minute intervals: 20mins (3A), 40mins (3B) and 60mins (3C). The background corrected uptake ratios of ICG in the various light exposure groups were calculated. A) 100J/cm^2 was 5-fold and 19.3 fold higher than 30J and 10J/cm^2 respectively, while 50J/cm^2 was 11.6-fold and 44.4-fold higher respectively. B) 100J/cm^2 was 22.2-fold and 43.9-fold higher than 30J and 10J/cm^2 respectively, while 50J/cm^2 was 16.3-fold and 32.2-fold higher respectively. C) 100J/cm^2 was 10.8-fold and 26.1-fold higher than 30J and 10J/cm^2 respectively, while 50J/cm^2 was 16.4-fold and 39.4 fold higher respectively. At all timepoints, no significant difference was observed between the 2 higher light exposure groups of 100J and 50J/cm^2 suggesting that a light dose of 50J/cm^2 is optimal for the permeability and retention effect leading to a higher leakage and uptake of ICG into the tumor bed. Key: † - marginally significant, ***** $p<0.05$, ****** $p<0.01$

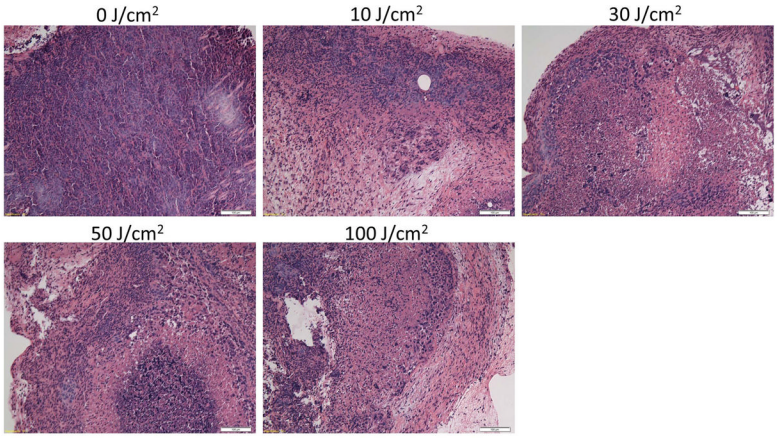

Figure 5.

Histological pictures of A431 tumors, which were treated with PIT at 0, 10, 30, 50 and 100J/cm2 sections are shown. All specimens were stained with hematoxylin and eosin. Microscopic evaluation of PIT-treated tumors revealed diffuse necrosis and micro-hemorrhage with scattered clusters of damaged tumors cells after higher exposure of NIR light, 50 and 100J/cm2. At the highest light exposure group, 100J/cm2, necrotic damage was more intense and fewer tumor cells remained. In contrast, when only 10J/cm2 of NIR light exposed, necrotic cell damage was found in only limited areas within the tumor while substantial amounts of healthy cancer foci remained. Cancer cell damages in tumor after varying doses of NIR light exposure correlated well to the kinetic changes which were detected by dynamic fluorescence imaging with ICG. Scale bars represent 100μm.